RESEARCH ARTICLE

Editorial Process: Submission:05/12/2025 Acceptance:30/08/2026 Published:27/09/2026

Anticancer and Bactericidal Activity of Manganese Ferrite Nanoparticles Synthesised by Using Allicin Extract

Sakthivel Muthu[1], Priyadharsani Vajjiravelu[2], Tanish Madhav Giridharan[3], Vanaja Mahendran[4]*, Bharathi Venkatachalam[5], Mythileeswari Lakshmikanthan[6], Shenbhagaraman Ramalingam[7]*

Abstract

Objective: The objective of this study is to synthesize manganese ferrite ($MnFe_2O_4$) nanoparticles (MnF NPs) using allicin extracted from *Allium sativum* and to assess their bactericidal and anticancer activities. **Methods:** Allicin from A. sativum was extracted using ethanol and confirmed by UV–visible spectrophotometer (λ max 240 nm). AMnF nanoparticles (Allicin-MnF NPs) synthesized via a co-precipitation route using allicin extract as reducing and stabilizing agent. The synthesized AMnF NPs were characterized using various instrumental techniques such as UV–vis absorption spectroscopy, FTIR, and SEM. Bactericidal activity was assessed by Agar well diffusion and MBC/MIC determination methods. Anticancer activity was examined against IMR-32 neuroblastoma cells and normal Vero cells using the MTT assay. **Results:** The synthesized AMnF NPs showed a distinct band in UV–vis absorption at 290 nm and FTIR bands characteristic of spinel ferrite metal–oxygen vibrations (555 cm^{-1}), along with organic functional groups from allicin. SEM analysis revealed agglomerated, near-spherical particles of 20–50 nm. The allicin extract exhibited notable bactericidal activity against Enterobacter sp and Staphylococcus aureus (MBC/MIC≤1.5), while showing bacteriostatic effects against Clostridium sp., Escherichia. coli, and Salmonella sp. The bactericidal behavior of the AMnF NPs depended on their concentration, with the highest action demonstrated against S. aureus and B. subtilis strains (100 µg/mL). Cytotoxic effects of NPs were dependent on concentration with an inhibitory concentration at 54.6 µg/mL, similar to doxorubicin at IC_{50} 46.33 µg/mL. Toxic effects on normal cells, such as Vero, were noted to be minimal at IC_{50} of >90 µg/mL. **Conclusion:** The nanoparticles synthesized with the help of allicin display efficient antibacterial and antitumor effects while being non-toxic to healthy cells.

Keywords: Allicin, Manganese ferrite nanoparticles, Scanning electron microscope, Bactericidal activity

Asian Pac J Cancer Prev, **27 (9)**, 3253-3263

Introduction

Natural plant-derived compounds possess a long history of application in managing diverse human health conditions. Nutritional factors significantly influence the onset of many human diseases, and certain foods are universally recognized as beneficial to human health, despite cultural variations in diet [1]. Garlic (*Allium sativum* L.), belonging to the Alliaceae family, ranks next to onion as one of the most extensively utilized Allium species and serves both culinary and medicinal purposes [2]. Its biological activities arise mainly from organosulfur constituents, including allicin (C6H10O2S), diallyl disulfide (C6H10S2), S-allyl cysteine (C6H11NO2S), and diallyl trisulfide (C6H10S3) [3]. This plant is consumed in several forms including fresh leaves, dried cloves, or as processed products such as essential oil, extracts, and powders each preparation influencing its overall bioactive profile [4].

Garlic contains a high proportion of allicin (2-propene-

*[1]Department of Dermatology, Saveetha Medical College and Hospital (SMCH), Saveetha Institute of Medical and Technical Sciences (SIMATS), Thandalam, Chennai-602105, Tamil Nadu, India. [2]Department of Forensic Medicine and Toxicology, Saveetha Medical College and Hospital (SMCH), Saveetha Institute of Medical and Technical Sciences (SIMATS), Thandalam, Chennai-602105, Tamil Nadu, India. [3]Saveetha Medical College and Hospital (SMCH), Saveetha Institute of Medical and Technical Sciences (SIMATS), Thandalam, Chennai-602105, Tamil Nadu, India. [4]Department of Radiology, Saveetha Medical College and Hospital (SMCH), Saveetha Institute of Medical and Technical Sciences (SIMATS), Thandalam, Chennai-602105, Tamil Nadu, India. [5]Department of Biotechnology, Saveetha School of Engineering, Saveetha Institute of Medical and Technical Sciences (SIMATS), Saveetha University, Thandalam, Chennai-602105, Tamil Nadu, India. [6]Department of ENT, Saveetha Medical College and Hospital, Saveetha Institute of Medical and Technical Sciences (SIMATS), Saveetha University, Thandalam, Chennai-602105, Tamil Nadu, India. [7]Department of ENT, Saveetha Medical College and Hospital, Saveetha Institute of Medical and Technical Sciences (SIMATS), Saveetha University, Thandalam, Chennai-602105, Tamil Nadu, India. *For Correspondence: shenbhagaraman@gmail.com, amvanaja@gmail.com*

1-sulfinothioic acid S-2-propenyl ester), which makes up about 70% of its organosulfur compounds [5–7]. Crushing or grinding garlic activates alliinase, which converts alliin into allicin [8]. Allicin possesses an extensive range of biological activities, together with antioxidant, bactericidal, antiviral, and antifungal properties [9, 10] and has been reported to aid in the management of hyperlipidemia, cancer, diabetes, atherosclerosis, and cardiovascular disease [10, 11]. Allicin also known to aid in controlling hyperlipidemia, cancer, diabetes, hypertension, atherosclerosis, and various cardiovascular conditions [12, 13].

The iron oxide groups having ferromagnetism properties called as ferrite materials [14]. Iron oxide incorporate with divalent metals like Mn, Mg, Zn, Cu, Ag, Co, and Ni and form metallic ferrite with spinel structure [15]. If the divalent manganese ion is doped on the surface of ferrite at nanoscale level is referred as manganese ferrite nanoparticles (MnF NPs). Manganese ferrite ($MnFe_2O_4$) nanoparticles represent a significant class of magnetic metal oxide nanostructures, valued for features like enhanced magnetic permeability, robust chemical resistance, and adjustable surface functionality [16, 17]. Compared with other ferrite-based materials, manganese ferrites (MnF NPs) display superior biocompatibility, which broadens their utility across fields such as catalysis, biomedical engineering, and pollutant remediation [18]. Among the various fabrication routes, biosynthesis approaches that employ plant-derived metabolites or natural biomolecules have attracted considerable attention because they avoid hazardous chemicals, offer low toxicity, and support sustainable nanomaterial production [19]. In this work, the use of allicin to generate $MnFe_2O_4$ nanoparticles provides a promising pathway that merges the principles of green chemistry with the desirable magnetic and catalytic behaviour of manganese ferrites [20]. This approach leverages the dual functionality of allicin as both a reducer and stabilizer promoting nanoparticle formation while preventing aggregation and imparting biocompatibility [21].

Current trends in nanomaterial production emphasize the use of plant-based metabolites and biomolecules to drive particle nucleation and stabilization, largely because these strategies avoid toxic reagents and remain cost-efficient [21, 22]. The allicin-mediated fabrication of MnF NPs integrates the advantages of green chemistry with the magnetic and catalytic functionalities of manganese ferrites. Here, allicin contributes to MnF NPs formation by initiating ion reduction while also acting as a surface-binding molecule that controls particle growth and stability [23]. This synergistic strategy not only offers a sustainable route for $MnFe_2O_4$ production but also yields multifunctional nanomaterials with promising applications in medicine, sensing, and environmental remediation advancing the field toward safer and more sustainable nanotechnology [24]. In this study, allicin is extracted from *Allium sativum* (garlic) by solvent extraction method. Structure of extracted allicin is confirmed by UV-vis spectrophotometer, and Fourier transform Infrared spectroscopy (FTIR). Furthermore, allicin is used to synthesis and characterization of manganese ferrite nanoparticles and evaluate its bactericidal and anticancer potential.

Materials and Methods

Materials used

Chemicals and reagents (analytical grade, 99% pure) used in the study were purchased from Sigma-Aldrich, India. Ethanol, Muller Hinton agar, Agar powder, sterile forceps, antibiotic discs, and LB broth. Media for culturing microorganisms are prepared in double distilled water

Collection of microorganisms

The bacterial strains of S. aureus, Clostridium botulinum, Enterobacter sp, Salmonella sp, and *E. coli*, were acquired from MTCC, India. Cultures were sub-cultured in sterile LB broth is used to determination of bactericidal effects.

Extraction and characterization of allicin from garlic

Peel and weigh garlic cloves (25 g). Crush or homogenize the cloves using a mortar and pestle or blender. Crushing activates alliinase and forms allicin. The homogenate is left at room temperature for 10–15 minutes to allow the transformation of alliin into allicin. After this step, 100 mL of chilled ethanol is introduced, and the mixture is stirred or gently shaken for about 30 minutes on ice or at 4 °C. The resulting suspension is filtered using Whatman No.1 filter paper or muslin cloth to acquire the liquid extract containing soluble allicin. Any remaining particulate matter in the extract can be cleared by centrifuging the solution at 10,000 rpm for 15 minutes in a cooling centrifuge (4°C). Allicin is unstable besides degrades quickly. So that, it is stored at –20°C in dark containers. Extracted allicin is characterized using UV-vis spectrophotometer to find the corresponding λmax value for allicin measured in different wavelength.

Synthesis of MnF NPs Using allicin

MnF NPs were prepared through a co-precipitation approach using allicin extract. Manganese nitrate tetrahydrate and iron (III) nitrate nonahydrate were mixed in distilled water (100 mL) at a 1:3 molar ratio and warmed to 70 °C with constant stirring. After the metal salts had fully dissolved, 10 mL of the allicin extract was introduced to assist the reduction process. The suspension was then alkalized by slowly adding 1 M sodium hydroxide until the pH reached 10, at which point the ferrite particles began to form. Following a two-hour reaction, the precipitate was rinsed out, centrifuged, and dried. The dried nanoparticles were then mixed with the allicin extract and stirred for 24 h at room temperature to let functionalization. Allicin functionalized manganese ferrite nanoparticles (AMnF nanoparticles) were then dried by calcining for 180 min at 670 °C in muffle furnace.

Characterization of AMnF Nanoparticles

The extracted allicin was analyzed using a UV–vis spectrophotometer to determine its λmax value within the wavelength of 200–700 nm. FTIR analysis was performed to identify the functional groups, with spectra recorded

between 4000 and 500 cm^{-1}. The structure of the green fabricated AMnF nanoparticles was studied using a scanning electron microscope (SEM).

Antibacterial activity of allicin

Agar well assay

The bacterial cultures used in this study were procured from MTCC examined via the diffused agar well method [25]. Muller-Hinton agar medium was autoclaved, cooled and melted, and around 20 millilitres were added to each Petri dish. A gel puncture was used to create a well with a diameter of 5 mm after the organisms used for the overnight growth test were moved over the agar medium. Following that, the well was filled with 25, 50, 75, and 100 µg/ml of allicin, followed by control disc (Ampicillin) was placed over the media and they were maintained in incubator for one day at 35°C. The diameter of the formed zone surrounding the wells were noted. All the experiments were followed three times for statistical analysis.

Determination of Minimum Inhibitory Concentration (MIC) and Minimum Bactericidal Concentration (MBC)

The Minimum Inhibitory Concentration (MIC) and Minimum Bactericidal Concentration (MBC) of the allicin extract was determined using the broth microdilution method.

MIC Determination

96-well containing sterile microtiter plates were used to perform a two-fold serial dilution of the test substance in Mueller-Hinton broth (MHB) to obtain final concentrations typically ranging from 25 µg/mL to 100 µg/mL, depending on the sensitivity of the test organisms. Each well was inoculated with 100 µL of standardized bacterial liquid culture (1×10^4 CFU/mL) and 100 µL of the different concentrated allicin extract.

Positive control (bacteria + broth without the allicin extract) and negative control (broth + allicin extract without bacterial suspension) were included. The MICs were calculated as the lowest dose of the allicin extract that is comparison to the control wells, showed no discernible bacterial growth (i.e., no turbidity) when the broths were allowed to incubation at 35°C for 18 hours.

MBC Determination

10 µL aliquots from the wells that did not exhibit any discernible bacterial growth (matching to the MIC and higher concentrations) were spread using L-rod on sterile NA (nutrient agar) plates and let incubated at 35°C for one day in order to estimate the MBC. The MBC, or 99.9% bacterial killing, was defined as the lowest concentration of the test material that totally suppresses the colony development on the agar surface. All experiments were conducted out in three separate trials, and the outcomes have been presented as the mean ± standard deviation (n=3).

Bactericidal activity of AMnF nanoparticles

Preparation of AMnF nanoparticles

For the antibacterial tests as well as the cytotoxicity tests, the concentration of the nanoparticles was calculated using the gravimetric analysis method. The nanoparticles were washed several times with distilled water, after which the nanoparticles were dried at 60 °C to a constant mass. The nanoparticles were suspended in a solution of sterile distilled water with a concentration of 1 mg/mL. The nanoparticles were subjected to ultrasonication for 20 minutes to ensure uniform dispersion. The nanoparticles were prepared from the stock solution with a concentration of 25, 50, 75, and 100 µg/mL.

Assessment of bactericidal activity of AMnF nanoparticles

The bactericidal activity of allicin-functionalized MnF nanoparticles was established against both Gram-positive (*Staphylococcus aureus*, *Bacillus subtilis*) and Gram-negative bacteria (Escherichia coli, Pseudomonas aeruginosa, Enterobacter sp) using the agar well diffusion assay. On the just sterilized Muller-Hinton Agar medium-containing plates, a freshly made bacterial suspension is swabbed. Using gel puncture, around four wells are created on the agar surface, and various AMnF NP concentrations (25, 50, 75, and 100 µg/mL) were supplemented to the wells. Following incubation for 24 h at 35°C, the diameter (mm) of the inhibitory zone was observed.

Anticancer Activity

Cell Culture and Treatment

The human cancer cell line IMR-32 was grown in Dulbecco's Modified Eagle Medium (DMEM) containing 10% fetal bovine serum (FBS) and 1% antibiotic solution. The cultures were maintained at 37 °C in a humidity incubator with 5% CO_2 level.

MTT assay

The MTT assay (3-(4,5-dimethylthiazol-2-yl)-2,5-diphenyl tetrazolium bromide) has been employed to determine cell viability. Simply, the cells were introduced into 96-well plates at a cell density of 1×10^4 cells per well and treated with different dosages of MnF NPs for 24 h.

Following the procedure, the medium used was replaced with serum-free medium including MTT, after which there was incubating for 4 hours at 37 °C in a CO_2 incubator. The testing procedure's fundamental principle is that metabolically engaged cells metabolize the yellow MTT reagent into purple crystals of formazan. The crystals were dissolved using DMSO, and absorbance has been reported at 570 nm. Untreated cells were used as the standard to calculate the nanoparticles' IC50 value. Doxorubicin served as the positive control. Every experiment was carried out three times.

$$\% \textbf{ Cell Viability} = 1 - \frac{\textbf{Absorbance For NPs Treated Cells}}{\textbf{Absorbance For Control Cells}} \times 100$$

Statistical analysis

The experimentally derived data were subjected to regression analysis to calculate the half-maximal inhibitory concentration (IC_{50}) for cell viability. All results are presented as mean ± SD, based on triplicate measurements from three separate experiments (n = 3). Significance tests of difference between the control (standard) and the AMnF nanoparticles were generated using a One-Way ANOVA

and then tested post hoc with a Tukey's Test (*p-value ≤ 0.05, **p-value ≤0.01).

Results

Characterization of Allicin extract and Allicin mediated MnF nanoparticles

UV- vis absorption

The UV–vis absorption spectrum of the allicin sample exhibited a prominent peak at approximately 240 nm, which is consistent with the characteristic absorption of allicin (Figure 1). Allicin, a thiosulfinate compound, absorbs in the UV region due to the presence of conjugated sulfur-oxygen (S=O) functional groups and unsaturated bonds (C=C).

The UV–vis absorption spectrum of manganese ferrite (AMnF) nanoparticles synthesized using allicin as a reducing and capping agent, as shown in the Figure 2, exhibits a prominent absorption peak at 290 nm. This strong absorption in the UV-vis region is characteristic of charge transfer transitions, particularly from oxygen ligands (O^{2-}) to metal ions (Fe^{3+} and Mn^{2+}), which are commonly observed in spinel ferrites. The peak also indicates the formation of $MnFe_2O4$ nanoparticles with well-developed spinel structures.

FTIR Analysis of AMNF NPs

FTIR spectrum of AMNF nanoparticles was measured at different wavenumber from 4500 – 500 cm^{-1} shown in Figure 3. O–H stretching vibrations are responsible for a widened peak observed at around 3365 cm^{-1}, indicating the presence of hydroxyl groups, most likely from water molecules or phenolic chemicals in the allicin extract. Peaks at 2922 cm^{-1} and 2851 cm^{-1} correspond to C–H stretching vibrations of aliphatic $–CH_2–$ and $–CH_3$ groups, indicating organic constituents of allicin. The band at 1552 cm^{-1} is characteristic of N–H bending or possibly C=C stretching in aromatic rings, while the 1409 cm^{-1} band may arise from C–N stretching of amines or deformation vibrations of methyl groups. A notable peak at 928 cm^{-1} can be associated with C–O stretching vibrations, typical of alcohols, ethers, or esters. Most importantly, the strong absorption band at 555 cm^{-1} is indicative of metal–oxygen (M–O) stretching vibrations, indicating the formation of

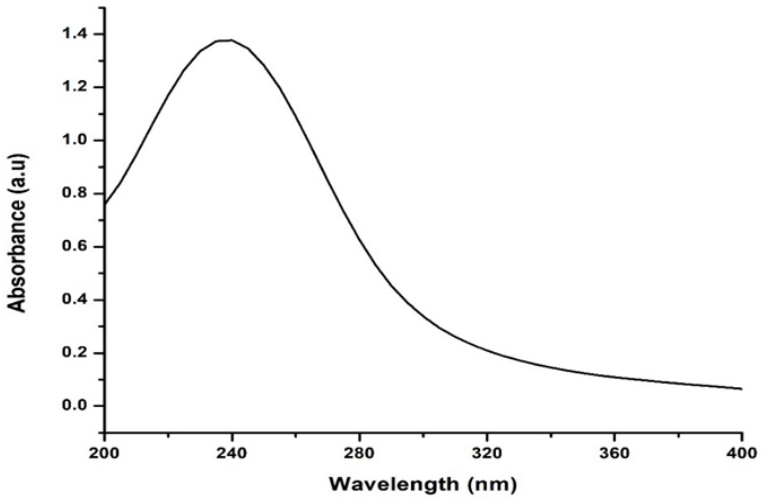

Figure 1. UV-vis Spectrum of Allicin Extracted from Garlic

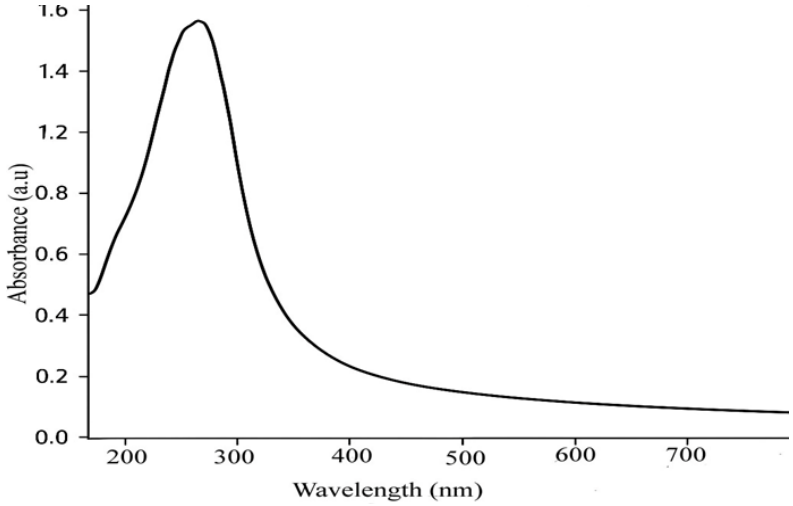

Figure 2. UV-vis Spectrum of Allicin Mediated Synthesized Manganese Ferrite Nanoparticles (AMNF NPs).

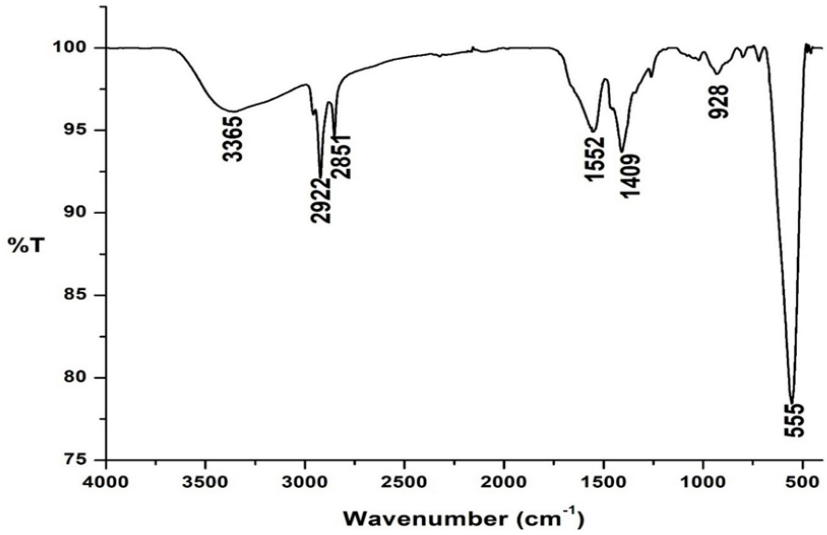

Figure 3. FTIR Spectrum of Green Synthesized AMnF Nanoparticles Using Allicin Extract

MnFe2O4 spinel structure. The successful generation of AMnF nanoparticles with bioactive chemicals from allicin serving as capping and reducing agents is confirmed by this spectrum.

SEM analysis

The scanning electron microscopy (SEM) image provided appears to show the surface morphology of AMnF (manganese ferrite) nanoparticles. The image reveals an agglomerated nanostructure with individual nanoparticle sizes roughly ranging between 20–50 nm and particles displaying irregular but generally spherical morphology (Figure 4).

Bactericidal Activity of allicin extract

The bactericidal activity of allicin extract was tested against five bacterial strains (Clostridium sp., Enterobacter sp., Escherichia coli, Salmonella sp., and *Staphylococcus aureus*) using the standard diffused agar well method at dosages of 25 µg, 50 µg, 75 µg, and 100 µg, alongside a control. Among the tested organisms, Enterobacter sp. exhibited the highest sensitivity, with the zone of inhibition increasing consistently across concentrations and reaching a maximum of 25.00 ± 0.47 mm at 100 µg. *Staphylococcus aureus* also responded strongly, displaying a concentration-dependent increase in inhibition, peaking at 19.33 ± 1.19 mm at 100 µg. Moderate inhibition was observed in Clostridium sp. and Salmonella sp., with maximum inhibition zone formation of 10.00 ± 0.47 mm and 11.33 ± 0.72 mm, respectively. *E. coli* showed the least sensitivity overall, with a noticeable increase only at the highest concentration, yielding a zone of 13.67 ± 0.72 mm. These results suggest a concentration-dependent antibacterial effect, with efficacy varying among bacterial species (Figure 5).

To further ascertain the potency of the antibacterial efficacy of allicin, the MIC and MBC were carried out using the broth microdilution technique. The MIC is the minimum concentration of the compound that can inhibit the growth of bacteria, whereas the MBC is the minimum concentration of the compound that can kill 99.9% of the microbial inhabitants. From the results, it was observed that the lowest values of MIC and MBC were recorded for Enterobacter sp. and *Staphylococcus aureus*, which indicated the highest level of sensitivity. However, the highest values of MIC and MBC were recorded for

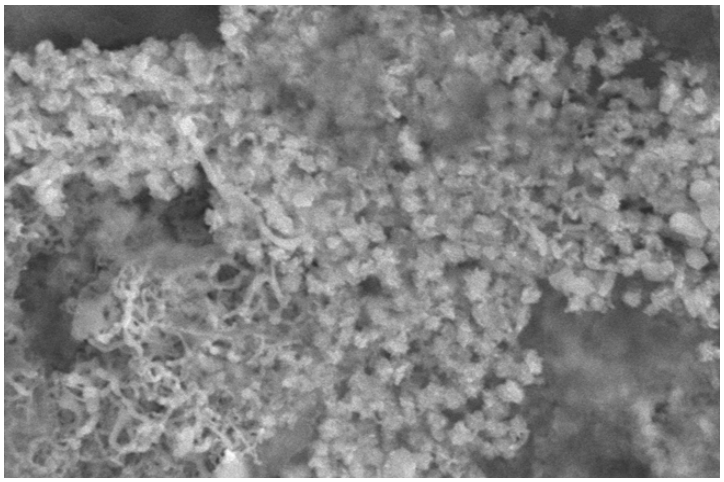

Figure 4. SEM Image of Green Synthesized AMnF Nanoparticles Using Allicin Extract Measured at 200 nm Scale Bar

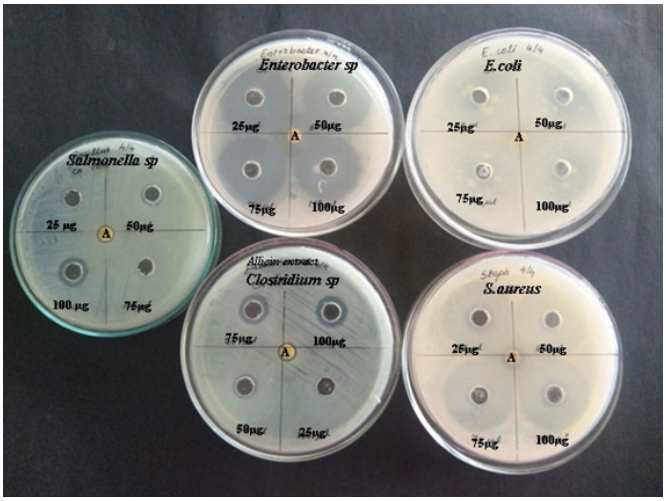

Figure 5. Zone of Inhibition (mm) Exhibited by the Allicin Extracted from Garlic at Different Concentrations (25 µg, 50 µg, 75 µg, 100 µg) against Five Bacterial Strains

Table 1. Zone of Inhibition (mm) Exhibited by the Test Substance at Different Concentrations (25 µg, 50 µg, 75 µg, 100 µg) against Five Bacterial Strains. Data represent mean ± standard deviation (n=3). The control group represents the inhibition observed with the active substance ampicillin.

Concentration	Clostridium sp	Enterobacter sp	*E. coli*	Salmonella sp	Staph. aureus
25µg	06.33±0.27	19.33±0.54	05.33±0.27	05.33±0.27	07.67±0.27
50µg	06.00±0.47	22.33±1.19	07.67±0.98	08.33±0.72	12.67±1.19
75µg	10.00±1.33	23.33±0.54	07.67±0.27	09.00±0.94	17.67±0.98
100µg	10.00±0.47	25.00±0.47	13.67±0.72	11.33±0.72	19.33±1.19
Control	06.33±0.27	14.67±0.54	05.47±0.27	06.72±0.27	08.54±0.27

E. coli, which indicated the highest level of resistance to the compound. The results are consistent with the results of the agar diffusion method, which indicated the dose-dependent antibacterial efficacy of the compound, which was bacteriostatic as well as bactericidal (Table 1).

Antibacterial action was interpreted based on the MBC/MIC ratio. In antimicrobial studies, when the MBC/MIC ratio is ≤4, it is considered bactericidal, while a ratio above 4 indicates a bacteriostatic action. In the present study, Enterobacter sp. had an MBC/MIC ratio of 1.0, and *Staphylococcus aureus* had an MBC/MIC ratio of 1.5, both close to unity, which indicates a strong bactericidal action of allicin on these organisms. In the case of Clostridium sp., Escherichia coli, and Salmonella sp., their MIC was within the tested range, while their MBC was above the tested concentration (>100 µg/mL). This indicates that these organisms were inhibited by allicin, not killed, within the tested concentration range, showing a bacteriostatic action of allicin on these organisms (Table 2).

Bactericidal activity of AMnF nanoparticles

The antibacterial activity of green synthesized MnFe2O4 nanoparticles using allicin extract is examined against bacteria *Bacillus subtilis, Staphylococcus aureus, Pseudomonas sp, Enterobacter sp and E. coli* (Figure 6). Herein, four different concentrations like 25, 50, 75 and 100 µg/ml are used to check the antibacterial activity (Table 3). In that, the 100 µg/ml concentration shows strong antibacterial activity in all aforementioned bacteria. Among the bacteria, *Bacillus subtilis* and S.aureus forms high zone of inhibition, which shows the MnFe2O4

Table 2. Minimum Inhibitory Concentration (MIC) and Minimum Bactericidal Concentration (MBC) and MBC/MIC Ratio of the Allicin against Selected Bacterial Strains

Bacterial strain	MIC (µg/mL)	MBC (µg/mL)	MBC/MIC ratio	Interpretation
Clostridium sp.	75	>100	>1.33	Bacteriostatic
Enterobacter sp.	25	25	1	Bactericidal
Escherichia coli	100	>100	>1.0	Bacteriostatic
Salmonella sp.	75	>100	>1.33	Bacteriostatic
Staphylococcus aureus	50	75	1.5	Bactericidal

Note: MIC represents the lowest concentration of allicin that inhibits visible bacterial growth, while MBC represents the lowest concentration that kills ≥99.9% of the bacterial population. The MBC/MIC ratio was calculated by dividing the MBC value by the MIC value. When the MBC exceeded the highest tested concentration (>100 µg/mL), the ratio was expressed as greater than the calculated value

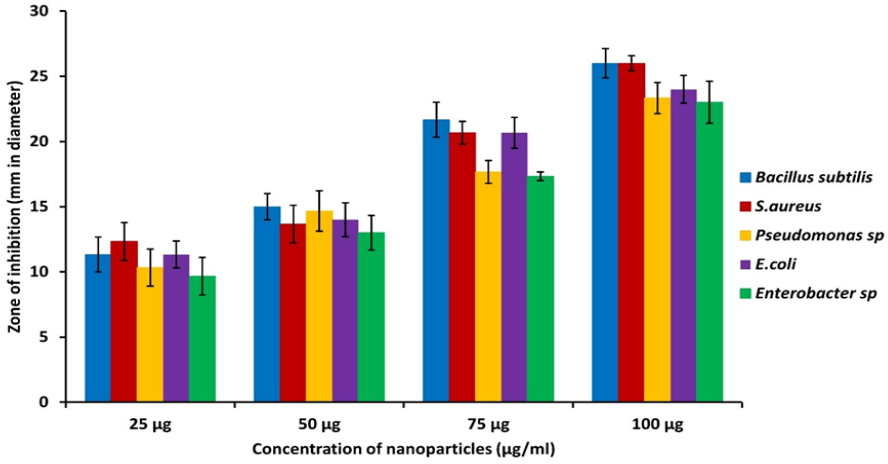

Figure 6. Antimicrobial Activity of AMnF Nanoparticles against Various Pathogenic Bacteria at Different Concentrations

Table 3. Antimicrobial Activity of AMnF Nanoparticles against Various Pathogenic Bacteria at Different Concentrations

Microorganisms	Zone of inhibition (mm in diameter)			
	25 µg/mL	50 µg/mL	75 µg/mL	100 µg/mL
Bacillus subtilis	11.33±1.34	15.00±1.01	21.67±1.33	26.00±1.13
S. aureus	12.33±1.45	13.67±1.45	20.67±0.88	26.00±0.58
Pseudomonas sp	10.33±1.41	14.67±1.54	17.67±0.88	23.33±1.24
E. coli	11.33±1.03	14.00±1.31	20.67±1.19	24.00±1.06
Enterobacter sp	09.67±1.45	13.00±1.33	17.33±0.33	23.00±1.61

nanoparticles e has high antibacterial activity against these two organisms.

Anticancer activity of AMnF nanoparticles

In vitro assessment of anticancer efficacy of AMnF nanoparticles against IMR-32 at different doses was examined by MTT assay (Figure 7). The MTT assay relies on the metabolic breakdown of MTT into formazan crystals following cancer cell line treatment. For IMR-32 cell lines, the inhibitory action of AMnF nanoparticles was contrasted with that of the conventional medication doxorubicin. Anticancer activity at the varied concentrations of 15 µg, 30 µg, 45 µg, 60 µg, 75 µg and 90 µg/ml exhibited efficient suppression against cancer cell lines. Figure 4 showed a progressive rise in the proportion of cell line inhibition through viability suppression across all treatments. However, against IMR-32 cancer cell lines, doxorubicin and nanoparticles at 90 µg/ml exhibit cell

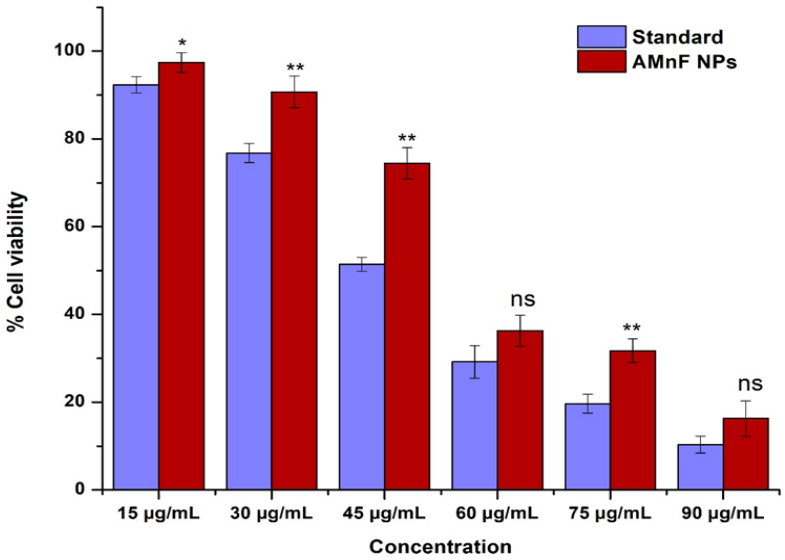

Figure 7. Anticancer Effector Activity of AMnF Nanoparticles against IMR-32 is Presented here. All statistical calculations were performed on the basis of the mean and standard deviation (n=3). Significance tests of difference between the control (standard) and the AMnF nanoparticles were generated using a One-Way ANOVA and then tested post hoc with a Tukey's Test (*p-value ≤ 0.05, **p-value ≤0.01).

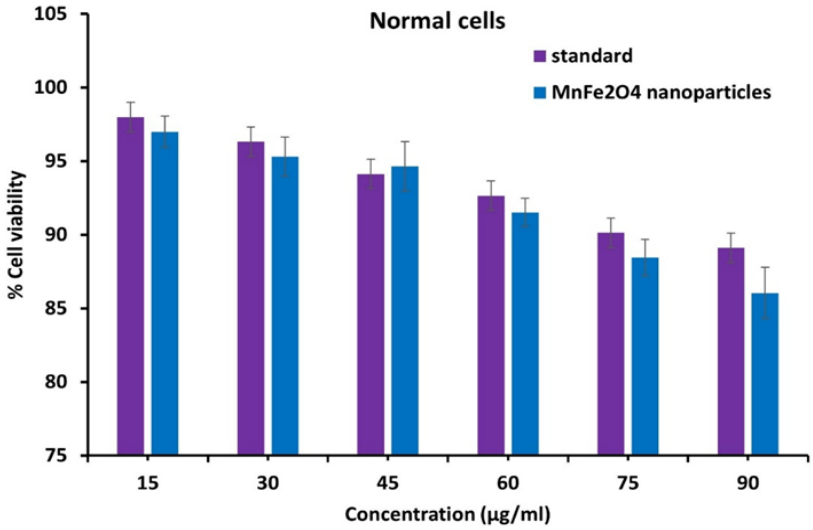

Figure 8. AMnF Nanoparticles' Effects on Typical Vero Cells. The values are given as mean ± SD (n = 3). One-way ANOVA and Tukey's post hoc test were used for statistical analysis. Variations were deemed statistically not significant.

viability of 10.89±1.14% and 16.05±1.13%, respectively. The IC_{50} value of the standard compound was 46.0 µg/mL, whereas AMnF nanoparticles exhibited an IC_{50} value of 54.6 µg/mL Statistical analysis revealed that the difference in cytotoxicity between the two treatments was significant ($p < 0.05$). In order to evaluate the biosafety of the compound, the cytotoxic effect of the AMnF nanoparticles was also investigated on normal vero cells. The results showed that the compound exhibited low toxicity with IC_{50} value > 90 µg/mL, thus demonstrating selective toxicity against cancer cells (Figure 8).

Discussion

The use of allicin a biologically active organosulfur compound derived from garlic not only aids in nanoparticle formation but also provides bio-functional properties [26], making these MnF nanoparticles suitable for biomedical or antimicrobial applications [27, 28]. This observation is in agreement with earlier reports where allicin showed maximum absorbance around 240–250 nm [29, 30]. Allicin mediated synthesized MnF nanoparticles shows SPR band at 290 nm indicates spinel structure. A single, sharp peak in the visible spectrum indicates a comparatively uniform nanoparticle size and effective allicin capping, which could aid in surface stabilization and passivation [31]. In accordance with the semiconducting nature of ferrite nanoparticles, the slow decline in absorbance after 300 nm suggests less light absorption in the visible spectrum [32]. The band observed at 555 cm^{-1} corresponds to metal–oxygen stretching vibrations characteristic of spinel ferrites [43]. This spectrum verifies that the synthesis of MnF nanoparticles was successful through biochemistry, where bioactive compounds of allicin acted as reducing agents and capping agents. The SEM image of MnF nanoparticles also indicates that clustering is occurring, showing strong interparticle interactions that could be due to magnetic dipole-dipole interactions and high surface energies, which are common properties of ferrite nanostructures [33]. The unique porous web structure of this material, which could increase its surface area significantly, also makes it suitable for adsorption and catalytic applications, according to Gnanaprakash et al. [34]. The synthesis of this nanostructured MnF material was also verified by SEM analysis [35]. This strong tendency of MnF nanoparticles to agglomerate could be due to magnetostatic interactions between these nanostructures, which is a common property of soft ferrimagnetic nanostructures. The aggregates formed by these nanostructures are useful in applications that need strong magnetic responses but could be disadvantageous in applications that need high surface area, such as adsorption and catalysis.

The bactericidal activity of the allicin extract of garlic was tested against Clostridium sp., Enterobacter sp., *E. coli*, Salmonella sp., and S. aureus. The results established a dosage-dependent inhibitory effect as evidenced by the increased size of the inhibition zones with increased dosage. The difference in sensitivity can be accounted for by previous studies that have shown that differences exist in the cell wall composition, selective permeability, and efflux mechanisms between Gram-positive and Gram-negative bacteria [36]. The maximum bactericidal activity against Enterobacter sp. and S. aureus is consistent with previous studies that have shown both Gram-negative opportunistic pathogens and Gram-positive staphylococci exhibit increased sensitivity to bactericidal agents. The high susceptibility is further corroborated by the bactericidal potential of allicin against Enterobacter sp. (MBC/MIC = 1.0) and S. aureus (MBC/MIC = 1.5) in this study. Enterobacter sp. and S. aureus have relatively lower MIC values (25 µg/mL) compared to other tested organisms. This implies that even trace concentrations of the compound can effectively inhibit growth. This is desirable for potential therapeutic or antimicrobial coating use. Salmonella sp., Clostridium sp.,

and *E. coli* have relatively high MIC and MBC values. The bacteriostatic nature of these organisms suggests a reduced level of sensitivity. The defense mechanisms that these organisms use against the tested compound could be biofilm formation and enzymatic degradation of the active compound. Another possibility is the alteration in porin channels.

These results, therefore, clearly indicate that the test material possesses bactericidal as well as bacteriostatic properties, thus promising its potential as an antimicrobial compound. The wide spectrum of antimicrobial activity, as observed in the present study, indicates that these formulations may be employed for controlling both Gram-positive as well as Gram-negative microorganisms. In particular, the compound's strong bactericidal activity against Enterobacter sp. and *Staphylococcus aureus* indicates its potential as a potent compound for controlling these microorganisms. On the contrary, the relatively higher MIC and MBC values for Salmonella sp., Clostridium sp., and *Escherichia coli* indicate relatively lower sensitivities for these microorganisms, thus implying that relatively higher concentrations may be needed for exerting complete bactericidal effects on these organisms. In addition, these results may also indicate that a synergistic approach, involving a combination of this compound with membrane-permeabilizing agents or other antimicrobial compounds, may further enhance its bactericidal potential.

Recent studies have shown that natural compounds, especially antimicrobial agents and their nano-formulations from plant sources, have shown appreciable antibacterial potential against multidrug-resistant bacteria [37]. The increased biological potential of the AMnF nanoparticles over allicin can be explained by the unique physical and chemical properties of the nanoparticle system. The small size of the nanoparticles offers a greater surface area that can interact effectively with the cell membrane and increase the rate of cellular uptake [19]. Nanoparticle surfaces can act as carriers for the antimicrobial agent allicin. The nanoparticle carrier system enhances the stability of allicin, protecting it from quick degradation under physiological conditions. The encapsulation of allicin in the nanoparticle matrix enables the controlled release of the active component, thus enhancing the longevity of the antimicrobial action. The improved antimicrobial activity of nanoparticle-loaded allicin in comparison to free allicin can be explained in terms of enhanced uptake, stability of the bioactive component, and controlled release kinetics. This nanocarrier-mediated approach can offer a possible solution for the treatment and control of infections by both Gram-positive and Gram-negative bacteria [20].

Mechanistically, the bioactive compounds may act against disease causing bacteria via various mechanisms like cell membrane disruption, interference with crucial metabolic processes, inhibition of quorum sensing, or induction of oxidative stress (ROS). The reduced MIC and MBC values for Enterobacter sp. and *Staphylococcus aureus* also point towards the bactericidal activity of the phytocompound against those pathogens. This suggests that the antibacterial effect of the compound may also be concentration- and species-dependent. Some of the natural antibacterial compounds have been found to exhibit potent bactericidal and anti-biofilm activities against *Staphylococcus aureus*, including methicillin-resistant *Staphylococcus aureus* (MRSA), making them promising compounds for the treatment of infections caused by these pathogens [38, 39]. On the other hand, *Salmonella sp., Clostridium sp., and Escherichia coli* showed relatively moderate sensitivity, as evidenced by relatively higher MIC and MBC results. This may be due to the predominantly bacteriostatic action of the tested compounds. This finding is in line with the present research trends that indicate the potential value of plant-derived bioactive compounds and their nanoparticle-based formulations for the development of green therapy for antibiotic resistance.

Moreover, the MTT assay outcomes revealed that the synthesized manganese ferrite nanoparticles exhibited substantial cytotoxicity against IMR-32 neuroblastoma cells in a dose-dependent manner. The increased cytotoxicity of the synthesized nanoparticles could be explained by enhanced uptake of nanoparticles by cells, increased release of bioactive compounds, and increased interaction of nanoparticles with intracellular targets. Nanoparticle-based delivery systems are also reported to prevent the degradation of bioactive compounds, thereby increasing their half-life [40, 41]. The cytotoxicity of AMnF nanoparticles could be related to nanoparticle-induced oxidative stress that activates various pathways of apoptosis. Ferrite-based nanoparticles are reported to increase ROS generation inside cells, which may cause disruption of normal cellular functions through damage to critical biomolecules such as DNA, proteins, and lipids. This overproduction of ROS can affect mitochondrial functions, leading to a loss of mitochondrial membrane potential and the initiation of apoptosis-related signalling pathways. In addition, the uptake of nanoparticles by cancer cells may initiate mitochondrial-mediated apoptosis, leading to nuclear condensation and cell death. All these processes are responsible for the observed cytotoxic effects of the synthesized AMnF nanoparticles [42, 43]. This is in line with previous observations that have indicated that nanoparticle-mediated delivery of chemotherapeutic agents can significantly improve anticancer potency compared to free agents. Future studies should be directed towards comparing the cytotoxic potency of free allicin and nanoparticle-functionalized allicin systems in order to understand their synergistic anticancer potency.

In conclusion, the work describes a green synthesis technique that uses garlic extract, which contains allicin, a naturally occurring organosulfur molecule, to create manganese ferrite nanoparticles. The magnetic characteristics of and the bio-reductive characteristic of a ferrite nanoparticles naturally occurring organosulfur molecule are combined in this work in a novel way. For the nanoparticles with a diameter between 20 and 50 nm, structural and morphological investigation confirmed the bio-functionalized surface of the particles. Excellent antibacterial qualities were demonstrated by the nanoparticles against a variety of microorganisms. By

contrast, the nanoparticles had the most inhibitory effects against *Bacillus subtilis* and *Staphylococcus aureus*. By contrast, the strongest inhibitory effects against Enterobacter sp. and S. aureus were shown by pure allicin extract. This study proves that nanoparticles are potent against specific strains of bacteria compared to others. The results for the anticancer tests showed that the nanoparticles exhibited excellent inhibitory effects against IMR-32 neuroblastoma cancer cells, proving that the nanoparticles possess excellent potential for acting as a drug against cancer. In addition, the nanoparticles exhibited excellent selectivity against normal Vero cells.

In conclusion, allicin-functionalized MnF nanoparticles inherit the benefits of magnetic metal oxide nanostructures, green chemistry, and phytochemicals. The MnF nanostructures are good candidates for future applications in cancer therapy, surface coatings for antimicrobial activity, and nanomedicine due to their confirmed antimicrobial activity and selective cytotoxicity against cancer cells. Further mechanistic studies on the subject will be required to progress towards practical applications.

Author Contribution Statement

All authors contributed equally in this study.

Acknowledgements

None.

Conflict of interest

The authors declare no competing interests.

References

1. Parekh J, Chanda S. In vitro antimicrobial activity of Trapa natans L. fruit rind extracted in different solvents. African Journal of Biotechnology. 2007 Mar 19;6(6):766.
2. Onyeagba RA, Ugbogu O, Okeke C, Iroakasi O. Studies on the antimicrobial effects of garlic (*Allium sativum* linn), ginger (zingiber officinale roscoe) and lime (citrus aurantifolia linn). African J Biotechnol. 2004;3:552-4. https://doi.org/10.5897/AJB2004.000-2108.
3. Alare K, Alare T, Luviano N. Medicinal importance of garlic and onions on autonomic nervous system. Clin Pharmacol Biopharm. 2020;9(4):204. https://doi.org/10.4172/2167-065X.1000204.
4. Amagase H. Clarifying the real bioactive constituents of garlic. J Nutr. 2006;136(3 Suppl):716S-25S. https://doi.org/10.1093/jn/136.3.716S.
5. Chyau CC, Mau JL. Release of volatile compounds from microwave heating of garlic juice with 2,4-decadienals. Food Chem. 1999;64(4):531-535. https://doi.org/10.1016/S0308-8146(98)00162-9.
6. Chen KQ, Lei HB, Liu X, Cao WJ. Mini-review: The health benefits and applications of allicin. Front Pharmacol. 2025;16. https://doi.org/10.3389/fphar.2025.1715922.
7. Torres Palazzolo C, Ramirez D, Locatelli D, Manucha W, Castro C, Camargo A. Bioaccessibility and permeability of bioactive compounds in raw and cooked garlic. J Food Compos Anal. 2018;70. https://doi.org/10.1016/j.jfca.2018.03.008.
8. Chan JY, Yuen AC, Chan RY, Chan SW. A review of the cardiovascular benefits and antioxidant properties of allicin. Phytother Res. 2013;27(5):637-46. https://doi.org/10.1002/ptr.4796.
9. Alam MK, Hoq MO, Uddin MS. Medicinal plant *Allium sativum* = a review. J Med Plants Stud. 2016;4(6):72-79.
10. Houshmand B, Mahjour F, Dianat O. Antibacterial effect of different concentrations of garlic (*Allium sativum*) extract on dental plaque bacteria. Indian J Dent Res. 2013;24(1):71-5. https://doi.org/10.4103/0970-9290.114957.
11. Eidi A, Eidi M, Darzi R. Antidiabetic effect of Olea europaea l. In normal and diabetic rats. Phytother Res. 2009;23(3):347-50. https://doi.org/10.1002/ptr.2629.
12. Singh R, Singh K. Garlic: a spice with wide medicinal actions. J Pharmacogn Phytochem. 2019;8(1):1349-1355.
13. Singh P, Singh J, Kumari S, Singh BR. Medicinal values of garlic (*Allium sativum* L.) in human life: An overview. Greener J Agric Sci. 2014;4:265-80. https://doi.org/10.15580/GJAS.2014.6.031914151.
14. Huq F, Saha D, Ahmed R, Mahmood Z. Ni-Cu-Zn ferrite research: A brief review. J Sci Res. 2013;5:215-34. https://doi.org/10.3329/jsr.v5i2.12434.
15. Desai HB, Hathiya LJ, Joshi HH, Tanna AR. Synthesis and characterization of photocatalytic $MnFe_2O_4$ nanoparticles. Mater Today Proc. 2020;21(4):1905-1910. https://doi.org/10.1016/j.matpr.2020.01.248.
16. Akhlaghi N, Najafpour-Darzi G. Manganese ferrite ($MnFe_2O_4$) nanoparticles: from synthesis to application—a review. J Ind Eng Chem. 2021;103:292-304. https://doi.org/10.1016/j.jiec.2021.07.043.
17. Jesudoss SK, Vijaya JJ, Kennedy LJ, Rajan PI, Al-Lohedan HA, Ramalingam RJ, et al. Studies on the efficient dual performance of $Mn_{1-x}Ni_xFe_2O_4$ spinel nanoparticles in photodegradation and antibacterial activity. J Photochem Photobiol B. 2016;165:121-32. https://doi.org/10.1016/j.jphotobiol.2016.10.004.
18. Hosny AA, El-Deeb B, Mohamed ZA, Hassan A, Kamel M, Elbeltagi S, et al. Green synthesis of Mn-doped iron oxide nanoparticles using sugarcane juice for magnetic hyperthermia applications. Sci Rep. 2025;15(1):28686. https://doi.org/10.1038/s41598-025-11998-5.
19. Jayandran M, Muhamed Haneefa M, Balasubramanian V. Green synthesis and characterization of manganese nanoparticles using natural plant extracts and its evaluation of antimicrobial activity. J Appl Pharm Sci. 2015:105-10. https://doi.org/10.7324/JAPS.2015.501218.
20. Chaudhari A, Taslim K, Desai H, Ghosh S, Bhatt R, Tanna A. Dye degradation and antimicrobial applications of manganese ferrite nanoparticles synthesized by plant extracts. Chemical Physics Impact. 2022;5:100098. https://doi.org/10.1016/j.chphi.2022.100098.
21. Majani SS, Veena MA, Hemanth Kumar CM, Setty PBS, Iqbal M, Shivamallu C, et al. Sustainable synthesis of iron-doped manganese oxide nanoparticles for effective photo-accelerated detoxification of tetracycline. Sci Rep. 2025;15(1):18081. https://doi.org/10.1038/s41598-025-97862-y.
22. Azqandi M, Ramavandi B, Nasseh N, Zaarei D, Fanaei F. Green synthesis of manganese ferrite magnetic nanoparticle and its modification with metallic-organic frameworks for the tetracycline adsorption from aqueous solutions: A mathematical study of kinetics, isotherms, and thermodynamics. Environ Res. 2024;256:118957. https://doi.org/10.1016/j.envres.2024.118957.
23. Srinivasan MK, Prasad M. Recent advances in tumor targeted polymeric nanoparticles for HNC treatment: Enhancing therapeutic efficacy via engineered and

biocompatible drug delivery systems. J Oral Biol Craniofac Res. 2025;15(6):1316-30. https://doi.org/10.1016/j.jobcr.2025.08.012.
24. Ranjith N, Rajesh T, Ryntathiang I, Behera A, Prasad M, Jothinathan M. In silico and in vitro study prediction of the anti-inflammatory activities of identified bioactive compounds from madhuca indica flower extract. Texila Int J Public Heal. 2025;13:911-25. https://doi.org/10.21522/TIJPH.2013.13.01.Art085.
25. Bauer AW, Kirby WMM, Sherris JC, Turck M. Antibiotic susceptibility testing by a standardized single disk method. Am J Clin Pathol. 1966;45(4_ts):493-496. https://doi.org/10.1093/ajcp/45.4_ts.493.
26. Cutler RR, Wilson P. Antibacterial activity of a new, stable, aqueous extract of allicin against methicillin-resistant Staphylococcus aureus. Br J Biomed Sci. 2004;61(2):71-74. https://doi.org/10.1080/09674845.2004.11732646.
27. Goodarz Naseri M, Saion E, Khalil Zadeh N. The amazing effects and role of PVP on the crystallinity, phase composition and morphology of nickel ferrite nanoparticles prepared by thermal treatment method. Int Nano Lett. 2013;3(1):19. https://doi.org/10.1186/2228-5326-3-19.
28. Varaprasad B, Kocharlakota R, Srinivas A. Structural and magnetic studies of nano-crystalline ferrites MFe_2O_4 (M = Zn, Ni, Cu, and Co) synthesized via citrate gel autocombustion method. J Supercond Nov Magn. 2017;30. https://doi.org/10.1007/s10948-017-4153-y.
29. Rabinkov A, Miron T, Konstantinovski L, Wilchek M, Mirelman D, Weiner L. The mode of action of allicin: Trapping of radicals and interaction with thiol containing proteins. Biochim Biophys Acta. 1998;1379(2):233-44. https://doi.org/10.1016/S0304-4165(97)00104-9.
30. Lawson LD, Wang ZJ. Allicin and allicin-derived garlic compounds increase breath acetone through allyl methyl sulfide: Use in measuring allicin bioavailability. J Agric Food Chem. 2005;53(6):1974-83. https://doi.org/10.1021/jf048323s.
31. Sarwar Allah D, Atif Y, Rehan U, Fouzia T, Shaista A. Allicin-capped silver nanoparticles (AgNPs): Synthesis, profiling, antioxidant, and biomedical properties. Nano Biomed Eng. 2024;16(3):370-85. https://doi.org/10.26599/NBE.2024.9290090.
32. Issa EH, Dhahri R, Massoudi J, Dhahri E, Bahri F, Khirouni K, et al. Study of the structural, electrical, dielectric properties and transport mechanisms of $Cu_{0.5}Fe_{2.5}O_4$ ferrite nanoparticles for energy storage, photocatalytic and microelectronic applications. Heliyon. 2023;9:e17403. https://doi.org/10.1016/j.heliyon.2023.e17403.
33. Giri SK, Das NN, Pradhan GC. Synthesis and characterization of magnetite nanoparticles using waste iron ore tailings for adsorptive removal of dyes from aqueous solution. Colloids Surfaces A Physicochem Eng Asp. 2011;389:43–9. https://doi.org/10.1016/j.colsurfa.2011.08.052.
34. Rani B, Ghosh S. Optimization of electrolytes for enhanced performance of $MnFe_2O_4$ nanoparticles-based supercapacitor electrode. Phys Scr. 2025;100:105921. https://doi.org/10.1088/1402-4896/ae0c6f
35. Srinivasan MK, Packirisamy V. Tailoring the capacitance performance of hierarchical nanostructured vanadium pentoxide nanoparticles with samarium doping for supercapacitor application. Chem Phys Lett. 2025;878:142387. https://doi.org/10.1016/j.cplett.2025.142387.
36. Ezealigo U, Ezealigo B, Aisida S, Ezema F. Iron oxide nanoparticles in biological systems: Antibacterial and toxicology perspective. J Colloid Interface Sci. 2021:100027. https://doi.org/10.1016/j.jciso.2021.100027.
37. Pouran F, Mahdavian A, Aghazadeh H, Navidinia M. Mini review: Antimicrobial agents based on natural compounds: The key to solving the current crisis. Arch Pediatr Infect Dis. 2024;12. https://doi.org/10.5812/apid-146195.
38. Ansari S, Jha RK, Mishra SK, Tiwari BR, Asaad AM. Recent advances in *Staphylococcus aureus* infection: Focus on vaccine development. Infect Drug Resist. 2019;12:1243-55. https://doi.org/10.2147/idr.S175014.
39. Intra J, Carcione D, Sala RM, Siracusa C, Brambilla P, Leoni V. Antimicrobial resistance patterns of Enterobacter cloacae and Klebsiella aerogenes strains isolated from clinical specimens: A twenty-year surveillance study. Antibiotics (Basel). 2023;12(4). https://doi.org/10.3390/antibiotics12040775.
40. Soetaert F, Korangath P, Serantes D, Fiering S, Ivkov R. Cancer therapy with iron oxide nanoparticles: Agents of thermal and immune therapies. Adv Drug Deliv Rev. 2020;163-164:65-83. https://doi.org/10.1016/j.addr.2020.06.025.
41. Yoonus J, Resmi R, Beena B. Evaluation of antibacterial and anticancer activity of green synthesized iron oxide (α-Fe_2O_3) nanoparticles. Mater Today Proc. 2021;46. https://doi.org/10.1016/j.matpr.2020.12.426.
42. Zúñiga-Miranda J, Guerra J, Mueller A, Mayorga-Ramos A, Carrera-Pacheco SE, Barba-Ostria C, et al. Iron oxide nanoparticles: Green synthesis and their antimicrobial activity. Nanomaterials (Basel). 2023;13(22). https://doi.org/10.3390/nano13222919.
43. Vani K, Hari Kumar N, Ravinder D, Naveena G, Sathish B, Sriramulu G. Rare earth Gd3+-substituted Co spinel nanoferrites structural, dielectric and magnetic properties. Chem Phys Impact. 2024;8:100585. https://doi.org/10.1016/j.chphi.2024.100585.

This work is licensed under a Creative Commons Attribution-Non Commercial 4.0 International License.